Front. Optoelectron. 2012, 5(3): 284–291
DOI 10.1007/s12200-012-0275-9

RESEARCH ARTICLE

Temperature effects on output characteristics of quantum dot white light emitting diode

Amin RANJBARAN (✉)

Faculty of Engineering, Islamic Azad University, Hamedan Branch, Hamedan 65138, Iran

Abstract In this paper, we proposed quantum dot (QD) based structure for implementation of white light emitting diode (WLED) based on InGaN/GaN. The proposed structure included three layers of InGaN QD with box shapes and GaN barriers. By using of single band effective mass method and considering strain effect, piezoelectric and spontaneous polarizations internal fields, then solving Schrödinger and Poisson equations self consistently, we obtained electron and hole eigen energies and wave functions. By evaluating dipole moment matrix elements for interband transitions, the output intensity was calculated due to the interband transition between two energy levels with highest emission probability. We adjusted QDs dimensions and material compositions so that the output light can be close to the ideal white light in chromaticity diagrams. Finally, effects of temperature variations on output spectrum and chromaticity coordinates were studied. We demonstrated that temperature variations in the range of 100 to 400 K decrease output intensity, broaden output spectral profile and cause a red shift in three main colors spectrums. This temperature variation deviates (x, y) are coordinated in the chromaticity diagram, but the output color still remains close to white.

Keywords quantum dot (QD), InGaN, optical intensity spectrum, white light emitting diode (WLED), chromaticity coordinate

1 Introduction

White light emitting diodes (WLEDs) have attracted an enormous attention in the field of solid state lighting and many efforts have been done to produce commercial WLEDs. Since the first high-brightness blue light-emitting diodes (LEDs) were introduced in the early 1990s [1,2], group-III-nitride semiconductors have gone a long way from being just promising materials in the industrial world to the basis for modern visible and ultraviolet (UV) optoelectronic devices. This is because of the unique physical properties of these semiconductors, namely, a direct bandgap that can be varied in a wide range from 0.65 to 6.2 eV, depending on the III-nitride alloy composition [3–5]. To realize WLEDs, two major schemes are normally proposed. The first one is using a wavelength converting layer, conventionally phosphorous, to produce long wavelengths via a red-shift in short wavelengths [6,7]. The second scheme is based on mixing red, green and blue colors (RGB) with a multi quantum well (QW) [8] or a multi quantum dot (QD) optoelectronic structures [9]. The first method has several disadvantageous, such as low efficiency, complexity of packaging and short lifetime due to the degradation of phosphor material [8]. Also, another drawback of first kinds of WLEDs method is the existence of energy Stokes shift [8,10]. The main problem behind the most LEDs based on InGaN/GaN quantum structures, which simultaneously emit several colors, is the lack of long wavelengths in the output intensity spectrum of these devices, at the visible range. In the color mixing method using an $In_xGa_{1-x}N$ nano-structure, an ideal white light cannot be created [11–14]. The reason of this problem is the high amount of In mol fraction within $In_xGa_{1-x}N$, that causes internal field to be increased and overlap between electron/hole envelop functions to be decreased in the long wavelength region of the visible range.

In this paper, we proposed an InGaN/GaN multi quantum dot WLED (MQD-WLED) structure, which emits red light with a desired intensity, where the output intensity spectrum will be close to the ideal white light.

First, eigen energies and wave functions for each layer of QD have been calculated using effective-mass approximation. From this obtained eigen energies and wave functions, dipole moment element matrix have been calculated and interband transitions have been decribed.

Received May 25, 2012; accepted June 11, 2012

E-mail: ranjbaran.amin9@gmail.com

Then optical gain (intensity) for each three QD layers would be evaluated. Second, important phenomenon in wurtzite crystals has been taken into account, such as strain, piezoelectric and spontaneous polarizations internal field, which have considerable effects on band structure and optical output intensity. Material composition and quantum box dimensions have been changed to study the obtained intensity of red, green and blue colors and chromaticity diagram of the output light. Finally, temperature variation effects on output intensity and Chromaticity coordinates have been investigated. The temperature has been varied from 100 to 400 K and its effects on RGB's output intensity and total spectrum of the output light have been studied.

The organization of this paper is as follows: In Section 2, the structure of MQD-WLEDs is described and a mathematical model based on self-consistent Schrödinger-Poisson equations solution is presented. In Section 3, simulation results using the given model in Section 2 are demonstrated and temperature effects on output light quality are presented. In Section 4, this paper ends with a brief conclusion.

2 MQD-WLED structure and theory

Schematic of the proposed vertically grown MQD-WLED, composed of three emitter layers, which are sandwiched between *p*-GaN and *n*-GaN layers, is illustrated in Fig. 1(a). This structure composed of three layers of quantum boxes that each layer emits a specific wavelength in the visible range (RGB spectrum). In this structure, the *p*-*n* junction is planned in the transverse direction, so that the lateral injection current causes a nearly uniform carrier concentration for all emitter layers [8]. The active region and barrier compositions are considered as $In_xGa_{1-x}N$ and GaN. QD shapes are supposed to be as a box, which is shown in Fig. 1(b). Distance between QDs in the laterally and vertically direction are so long that coupling between QDs can be ignored. To have such a MQD-WLED structure with uncoupled dots, we have to determine the distance between QDs of each layer, so that the wave functions between adjacent single QDs have no significant overlap. QD dimensions and material compositions for red, green and blue emission colors are presented in Table 1.

Effective mass equation has been used to calculate eigen energies, wave functions and relevant quantities. We start by considering the Schrödinger equation in the slowly varying envelope approximation in three dimensions as follows [15]:

$$\left\{\frac{-\hbar^2}{2m_i^*}\nabla^2_{x,y,z} + V_i(x,y,z)\right\}\psi(x,y,z) = E\psi(x,y,z), \qquad (1)$$

where m_i^*, $V_i(x,y,z)$ and $\Psi(x,y,z)$ are effective mass, overall potential distribution and the slowly varying envelope in different directions, respectively. The frequency range of

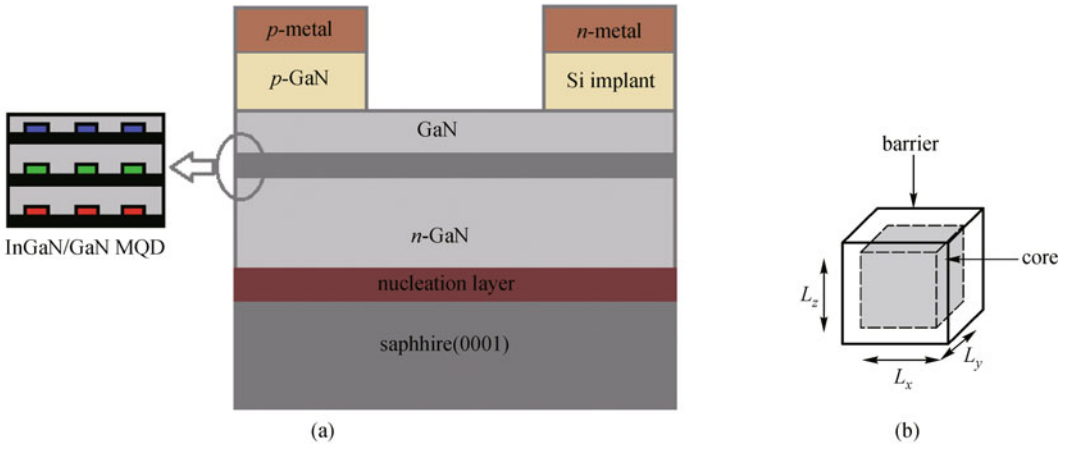

Fig. 1 (a) Schematic of MQD-WLED containing three emitters grown vertically, spacing between adjacent single QDs in the laterally and vertically direction is adjusted to minimize overlaps of corresponding wave functions; (b) proposed cubic shaped InGaN QD within a large GaN QD. L_x, L_y and L_z are quantum box dimensions

Table 1 QD dimensions and material compositions for red, green and blue emission colors

color	$L_x = L_y$ /nm	L_z/nm	barrier/dot	E_{c1}/eV	E_{hh1}	$E_{g,eff}$
red	10	3.1	$GaN/In_{0.33}Ga_{0.67}N$	1.5518	−0.4695	2.0213
green	10	3.2	$GaN/In_{0.26}Ga_{0.74}N$	1.8795	−0.4376	2.3171
blue	10	3.5	$GaN/In_{0.17}Ga_{0.83}N$	2.2918	−0.3965	2.6883

the visible light is so that we have to focus on interband transitions between conduction and valance bands.

One of the most important phenomenons in wurtzite nitride semiconductors is strain. The strain originates from the lattice mismatch between the heterostructure epilayers, such as InGaN/GaN. III-nitrides binaries InN > GaN > AlN, the order of lattice constant between adjacent layers is slightly different, and then strain will be an essential parameter should be taken in account during solving Schrödinger equation. The compressive strain shrinks the lattice bond and causes the charge center distortion that will create a dipole moment across the semiconductor nano-structure and will generate a strain-induced piezo-electric polarization ($\boldsymbol{P}_{\mathrm{PZ}}$). Another polarization effect which is called spontaneous polarization ($\boldsymbol{P}_{\mathrm{SP}}$), is due to the non-ideality of III-nitrides binary causing a relative shift of the anion and cation sublattices of the wurtzite structure and thus creates an additional nonzero dipole moment [16]. The overall polarization $\boldsymbol{P}$, in wurtzite-type semiconductors is given by

$$\boldsymbol{P} = \boldsymbol{P}_{\mathrm{PZ}} + \boldsymbol{P}_{\mathrm{SP}}. \tag{2}$$

This polarization induces an electrostatic potential φ, which can be obtained by first calculating the polarization charge density ρ, using [17,18]:

$$\rho = -\nabla \boldsymbol{P}, \tag{3}$$

and subsequently solving Poisson's equation,

$$\varepsilon_0 \nabla(\varepsilon_{\mathrm{r}} \nabla \varphi) = \rho, \tag{4}$$

where ε_0 and ε_{r} are the free space permittivity and dielectric constant of the semiconductor, respectively. The existing polarization in the InGaN/GaN material system will be taken in to account in the Schrödinger equation via the potential obtained from Eq. (4). Equations (1) and (4) should be solved self-consistently to obtain eigenvalues and wave functions. The equivalent effect of the polarization on eigenvalues and wave functions of electrons and holes can be regarded as internal electric field. In our structure, the internal field deviates electron and hole wave functions from QDs centers. This deviation decreases the overlap between electron and hole wave functions, then causes fall of optical output intensity in our investigated structure. In addition, this deviation reduces semiconductor effective bandgap, and a red shift in the emission spectra occurs.

As an example, Fig. 2 shows electron and hole wave functions corresponding to the first conduction and valance bands without and with internal field for blue emitting layer. As Figs. 2(a) and 2(c) demonstrate, the electron and hole wave functions are concentrated at the dot center. Figures 2(b) and 2(d) confirm up and down deviation of electron and hole wave functions from center of the QD due to the polarization induced internal field, respectively. These results are in a good agreement with Ref. [19].

Here, we are going to design a QD-WLED, with an output photoluminescence spectrum composed of three spectral wavelength peaks in the visible range (RGB). We varied quantum box dimensions and In mol fraction in the $\mathrm{In}_x\mathrm{Ga}_{1-x}\mathrm{N}$ to create three main colors. For red emitting QDs, the desired material is $\mathrm{In}_{0.33}\mathrm{Ga}_{0.67}\mathrm{N}$ with dimensions $L_x = L_y = 10$ nm and $L_z = 3.1$ nm. We focus on optical radiative transitions between conduction and heavy hole band, because the most radiative recombinations occur between first conduction level and first heavy hole level (e_1-hh_1) in a QD. The above red emitting QD gives us an effective bandgap equal to 2.0212 eV, $E_{\mathrm{hh1}} = -0.4695$ eV and $E_{\mathrm{c1}} = 1.5518$ eV. For green emitting QDs, the chosen active region composition is $\mathrm{In}_{0.26}\mathrm{Ga}_{0.74}\mathrm{N}$ with dimensions $L_x = L_y = 10$ nm and $L_z = 3.2$ nm. For this QD system, the values of energy subbands are $E_{\mathrm{c1}} = 1.8795$ eV and $E_{\mathrm{hh1}} = -0.4376$ eV yielding a 2.3172 eV energy band gap, which is the best appropriate for green emission. Finally, in order to design a blue emitting QD, the active region composition is chosen to be $\mathrm{In}_{0.17}\mathrm{Ga}_{0.83}\mathrm{N}$ with dimensions $L_x = L_y = 10$ nm and $L_z = 3.5$ nm. For this QD system, the values of energy subbands are $E_{\mathrm{c1}} = 2.2918$ eV and $E_{\mathrm{hh1}} = -0.3965$ eV yielding a 2.6883 eV energy band gap, which is the best appropriate for blue emission. In our simulation, the QDs are self-assembled on the GaN substrate, accompanied by a 0.5 nm InGaN wetting layer and is surrounded by 8 nm GaN barrier. In designing RGB QDs, we varied In mol fraction and QD sizes. By ascending amount of In mol fraction x in $\mathrm{In}_x\mathrm{Ga}_{1-x}\mathrm{N}$, strain and total internal field increase, in result wave functions overlap will decrease. But, as the effect of decreasing of overlap value which caused by an increase in QD dimension is more, so for longer wavelength emitter design, we used more In mol fraction x with small quantum box dimension. Therefore, the decrease of overlap between electron and hole wave functions due to the increase in In mol fraction x will be compensated with decreasing of quantum box dimensions. Because of all above features, for creation of red light with appropriate intensity in comparison with the blue light, we have chosen higher In mol fraction x and lower quantum box dimensions.

The linear optical gain of a QD in the active region is given as [20,21]

$$g(E) = \frac{2\pi e^2 \hbar N_{\mathrm{d}}}{c n_{\mathrm{r}} \varepsilon_0 m_0^2} \sum_{c,v} \frac{|P_{c,v}|^2}{E_{cv}} \int_{-\infty}^{+\infty} [f_c(E') - f_v(E')] \cdot G(E' - E_{cv}) B_{cv}(E - E') \mathrm{d}E', \tag{5}$$

where, N_{d} is the inverse of the crystal volume $N_{\mathrm{d}} = V^{-1}$. n_{r}, $\hbar$, E_{cv}, $P_{c,v}$, c, e and m_0 are refractive index, Plank constant divided by 2π, energy of interband transition, transition matrix element, speed of light, the free electron charge and mass, respectively. Indexes c and v represent discrete energy states in the conduction and valence bands, respectively. $G(E) = \delta(E)$, where $\delta(E)$ is the Dirac delta

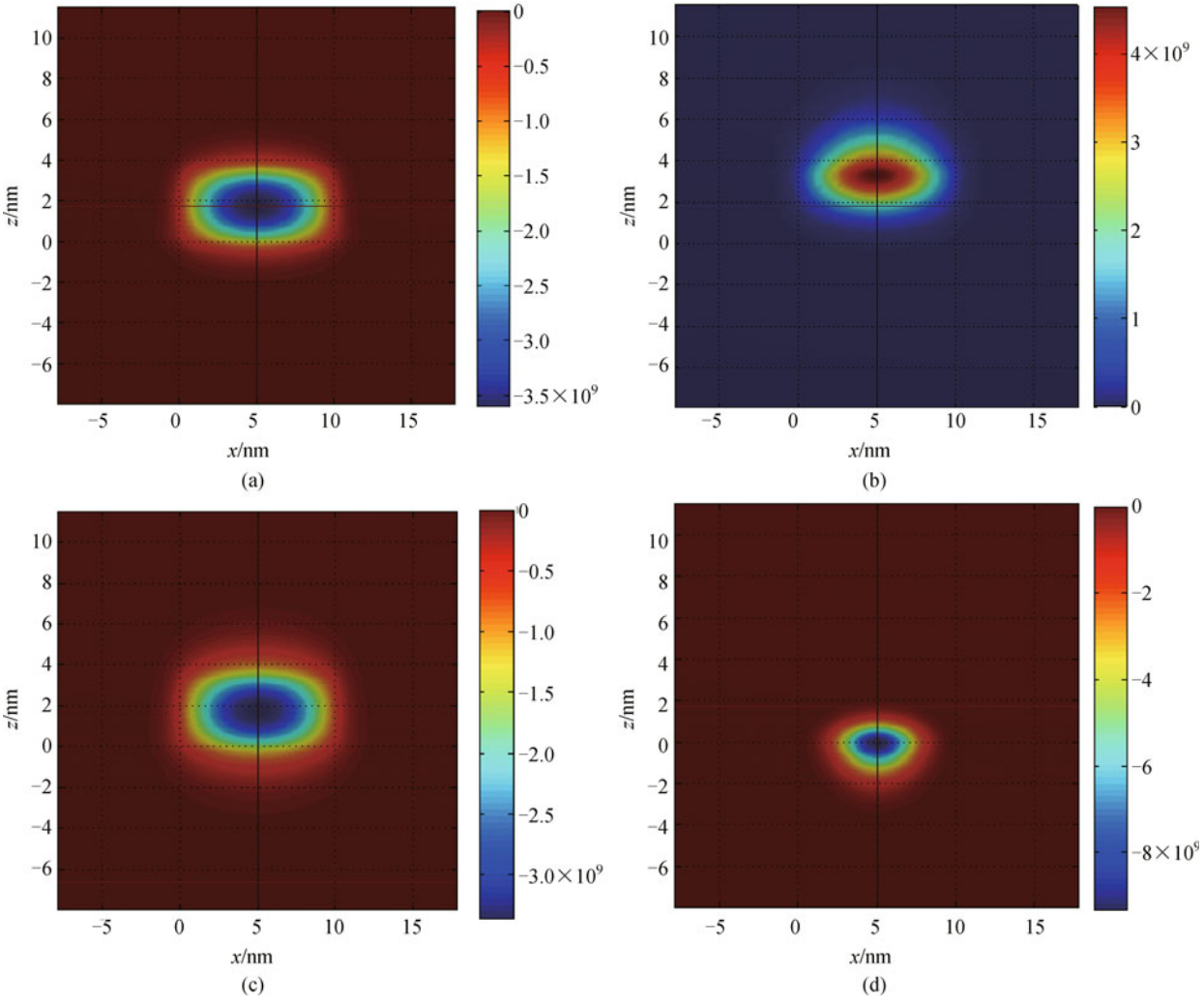

Fig. 2 Wave functions corresponding to the first conduction band, (a) without internal field and strain effects, (b) with internal field and strain effects, and heavy hole band, (c) without internal field and with strain effects, (d) with internal field and strain effects, for the blue color emitter. Deviation from dot center is obvious. Deviation of electron and hole wave functions from QD center, which decrease overlap between the electron and hole wave functions

function, and $f_c(E')$ and $f_v(E')$ are Fermi-Dirac distribution functions of the conduction-band and valence band, as [21]

$$f_i = \frac{1}{\exp\left(\frac{E_i - E_{f_i}}{k_B T}\right) + 1}, \quad i = c,v, \tag{6}$$

where E_{f_i} is the quasi-Fermi level, k_B is the Boltzmann's constant, and T is temperature in Kelvin. The values of E_{f_c} and E_{f_v} are determined from the following relations [22]:

$$N = \sum_i \frac{2}{\left[1 + \exp\left(\frac{E_i - E_{f_c}}{k_B T}\right)\right] l_x l_y l_z}, \tag{7(a)}$$

$$P = \sum_i \frac{2}{\left[1 + \exp\left(\frac{E_{f_v} - E_i}{k_B T}\right)\right] l_x l_y l_z}, \tag{7(b)}$$

where N and P, are electron and hole densities ($N \approx P$), respectively. l_x, l_y and l_z are quantum box dimensions along the x, y and z directions.

We take a Lorentzian distribution function for B_{cv} as [20]

$$B_{cv}(E - E') = \frac{\frac{\hbar \Gamma_{cv}}{\pi}}{(E - E')^2 + (\hbar \Gamma_{cv})^2}, \tag{8}$$

where $\hbar \Gamma_{cv}$ represents the inhomogeneous broadening due to the interaband scattering relaxation time τ ($\Gamma_{cv} = 1/\tau$). We can adjust the interband relaxation time τ to tune the half linewidth of the Lorentzian function $1/\tau$, which is

commonly on the order of $(ps)^{-1}$ for wurtzite crystals [5].

The transition matrix element is evaluated using the following relation [5]:

$$|P_{c,v}|^2 = \frac{3}{2} O_{ij} (M_b^{TE})^2, \tag{9}$$

where O_{ij} is the wave function overlap integral and M_b^{TE} is the dipole moment element. Bulk dipole moments for TE polarization is given by [5]

$$(M_b^{TE})^2 = \frac{m_0}{6}\left(\frac{m_0}{m_e^z} - 1\right)\frac{(E_g + \Delta_1 + \Delta_2)(E_g + 2\Delta_2) - 2\Delta_3^2}{E_g + 2\Delta_2}, \tag{10}$$

where m_e^z is the electron effective mass parallel to the QD growth direction. Δ_1 is the crystal-field split energy, $\Delta_2 = \Delta_3 = \Delta_{so}/3$, and Δ_{so} is spin–orbit split energy.

We use Eq. (5) to calculate optical gain spectrum for each set of QDs illustrated in Fig. 1. The material parameters used in our simulations can be found in Table 2.

Table 2 Wurtzite GaN-family QD parameters, which are used in our calculations

parameters	InN	GaN	AlN
m_e^z/m_0	0.07	0.2	0.3
Δ_{cr}/eV	0.040	0.010	−0.169
Δ_{so}/eV	0.005	0.017	0.019
E_g/eV	0.76	3.44	6.28
lattice constant a/Å	3.54	3.19	3.11

3 Results and discussion

Figure 3 demonstrates active layer optical intensity due to interband transition between hh_1-el_1 for three layers of QDs. This intensity is obtained at carrier injection of $1 \times 10^{19}\,cm^{-3}$ and temperature $T = 300\,K$. The given parameters in Table 1 are so adjusted that all emitting layers generate almost equal light intensity, which is evident from Fig. 3. Combining these narrow blue, green and red spectrums gives us a spectrum, which is close to white light. Quality of this white light is measured comparing with chromaticity diagram, which is shown in Fig. 4. This chromaticity coordinates calculated based on the standard observer CIE 1931 color matching functions [23]. The peak amplitudes of RGB colors have been so adjusted that resulted coordinate in the chromaticity coordinate diagram is $(x, y) = (0.3438, 0.3465)$, which is very close to the (0.33, 0.33) coordinate of ideal white light with a flat spectrum.

An important parameter, which affects on quality of generated white light of QD-WLED, is temperature. Variations in temperature displaces (x, y) in the chromaticity diagram. Figures 5(a), 5(b) and 5(c) show effects of

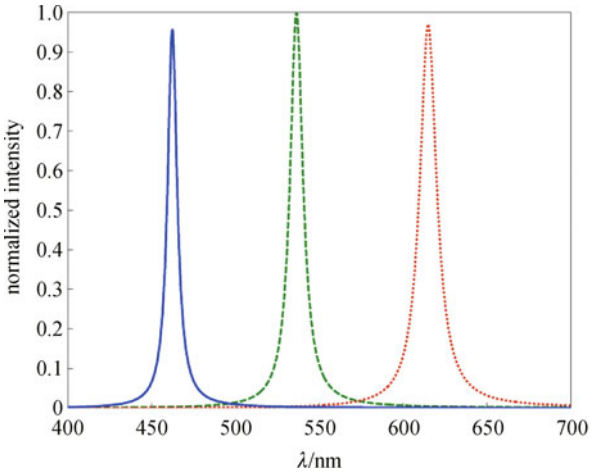

Fig. 3 Output intensity for three light emitting layers of blue, green and red QDs at the temperature $T = 300\,K$

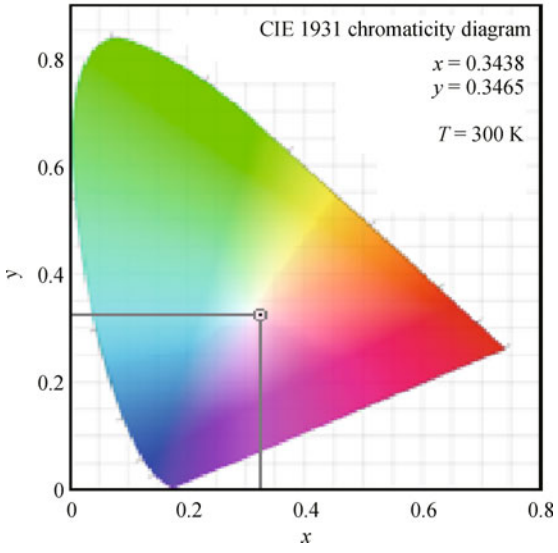

Fig. 4 QD-WLED output white light coordinate in standard chromaticity diagram

temperature variations on red, green and blue output intensities, respectively. As temperature increases from 100 to 400 K, a redshift in output intensity happen, in addition, amplitude of the intensity peak is going to decrease, for three sets of RGB colors. The redshift in output spectrum happens because a decrease on the effective bandgap occurs when temperature increases. As temperature increases, the energy gap of semiconductors decreases. The temperature dependence of the energy gap of a semiconductor can be expressed by the following formula:

$$E_g(T) = E_g(T = 0) - \frac{\alpha T^2}{T + \beta}, \tag{11}$$

where E_g denotes the energy gap at temperature T, and α

and β are fitting parameters. The constants α and β are considered, in principle, to be dependent on the sample compositions. The values of α and β were evaluated from the linear interpolation from the values for GaN and InN.

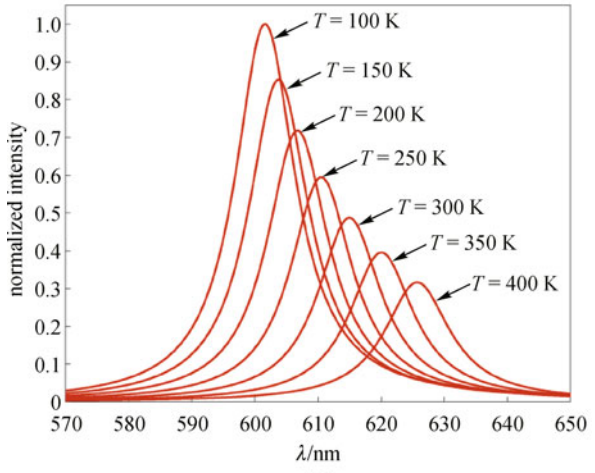

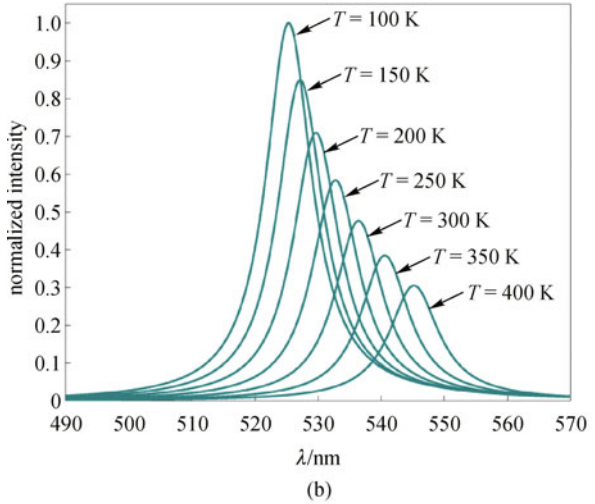

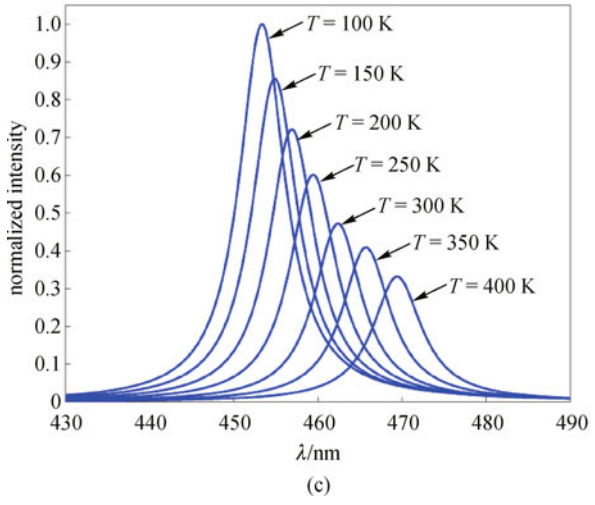

Fig. 5 Temperature increasing effects from 100 to 400 K for emitter of (a) red; (b) green; (c) blue

According to this equation by increasing of temperature, effective bandgap will decrease, which is in turn responsible for redshift of the RGB spectrums versus temperature.

Another property, which is observed in Figs. 5(a), 5(b) and 5(c), is shrinking of output spectrum peak with temperature increase. Reduction in output intensity peak with temperature confirms that the strong confinement of carriers in InGaN QDs at lower temperatures will be weak at higher temperatures. By increasing temperature, electrons and holes in E_{c1} and E_{hh1} are pushed to higher energy subbands in the conduction and valance bands, respectively, then a reduction in first level carriers take places. On the other hand, since electrons and holes are pushed aside, by internal electric field to the top and to the bottom of dots in z-direction, accordingly. As temperature increases the carriers spread in QDs, so the probability of their trapping at nonradiative recombination centers increases, in result intensity peak amplitude will decrease.

Here, we investigate variations of output power spectral density with respect to temperature changes. The power spectral density is given by [24]

$$P(\lambda) = \frac{\hbar\omega}{\tau_{ph}} N, \tag{12}$$

where $\hbar\omega$, N are photon energy and number of photons, respectively. Also the total output optical power emitted by a light source is given by [25]

$$P = \int_{\lambda} P(\lambda) \mathrm{d}\lambda. \tag{13}$$

Figure 6 demonstrates normalized output power spectral density for different values of temperature. As seen from it, for a 100 K increase in temperature, the peak of the output power spectrum for each color experiences almost 25% decrease. It should be noted that the photons of the blue

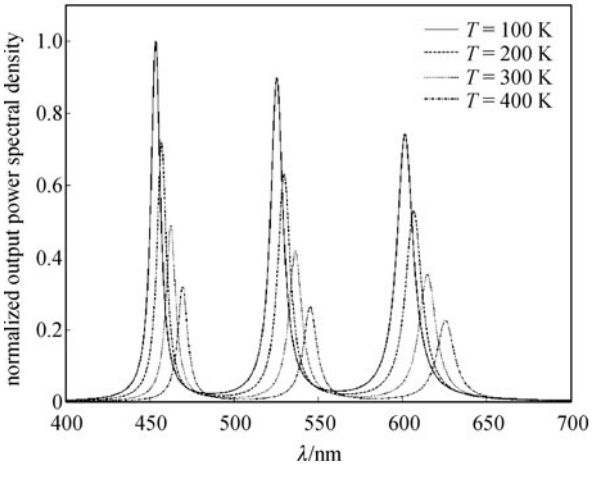

Fig. 6 Normalized output power spectral density for different values of temperature

light comprise more energy than green and red colors; furthermore the peak of the blue color output power density is greater than green and red colors. Comparing Figs. 6 and 3, we find that higher peak in intensity and power can appear in different wavelengths. Figure 7 shows normalized output optical power vs temperature.

Figure 8 demonstrates effects of temperature variations on chromaticity coordinates for QD-WLED structure of Fig. 1. When temperature increases, x and y values follow the path, which is illustrated in Fig. 8. Using this figure, we claim that the output light quality, by temperature variation, will not deviate from white light, considerably. This can be explained by using Fig. 5. As seen from Figs. 5(a) to 5(c), by temperature increasing, red, green and blue spectrums experience almost equal redshift and intensity fall, simultaneously. The amount of this red shift by temperature is such that these main colors spectrums do not come out of the red, green and blue regions, so temperature variations dose not move much away the output light from the standard white light.

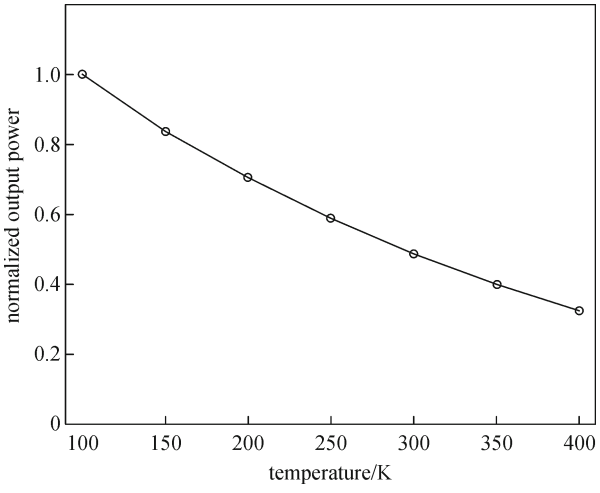

Fig. 7 Effects of temperature variation on normalized optical output power

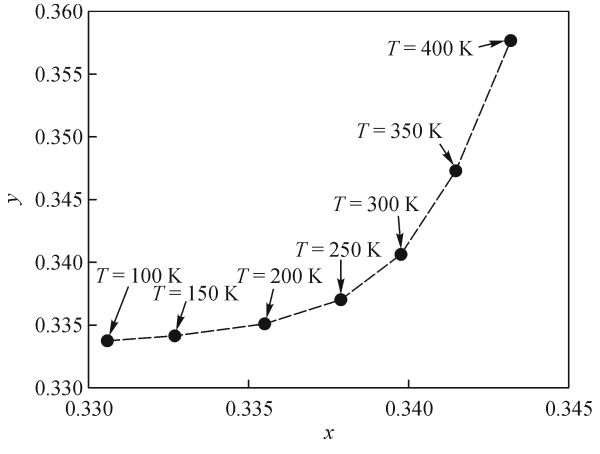

Fig. 8 Effects of temperature variation from 100 to 400 K on chromaticity coordinates for proposed structure

4 Conclusions

In this paper, a QD-WLED structure based on three layers of QDs was designed and analyzed. These layers were adjusted that each layer emits one of the RGB colors in the visible range. QD sizes and materials compositions were chosen in such a way that the output intensity spectrum of these three layers results a light, which is much close to the ideal white light in the chromaticity diagram. To calculate the eigen energies and wave functions of electrons and holes, we used single band effective mass method. Then, we took in account strain effects and piezoelectric and spontaneous polarization internal fields in our calculation. Output intensity and power of RGB QDs were calculated regarding interband transition between two energy levels that have highest radiative transitions. The peak amplitudes of RGB colors were such that the resulted coordinate in chromaticity diagram is $(x, y) = (0.3438, 0.3465)$, which is very close to the (0.33, 0.33) coordinates of ideal white light in a standard wide spectrum. We depicted the effects of temperature change on output intensity, spectrum profile and show that temperature variation from 100 to 400 K decrease output intensities, broaden output spectral profile and cause a redshift in RGB spectrums. This temperature variation slightly deviates (x, y) coordinate in the chromaticity diagram, so that the output color remains close to white.

References

1. Nakamura S, Mukai T, Senoh M. Candela-class high-brightness InGaN/AIGaN double-heterostructure blue-light-emitting diodes. Applied Physics Letters, 1994, 64(13): 1687–1689
2. Nakamura S. Zn-doped InGaN growth and InGaN/A1GaN double-heterostructure blue-light-emitting diodes. Journal of Crystal Growth, 1994, 145(1–4): 911–917
3. Vurgaftmana I, Meyer J R, Ram-Mohan L R. Band parameters for III–V compound semiconductors and their alloys. Journal of Applied Physics, 2001, 89(11): 5815–5875
4. Wu J, Walukiewicz W, Yu K M, Ager J W, Haller E E,Lu H, Schaff W J. Small band gap bowing in $In_{1-x}Ga_xN$ alloys. Applied Physics Letters, 2002, 80(25): 4741–4743
5. Piprek J. Nitride Semiconductor Devices: Principles and Simulation. NewYork: WILEY-VCH, 2007
6. Allen S C, Steck A J. A nearly ideal phosphor-converted white light-emitting diode. Applied Physics Letters, 2008, 92(14): 143309–143311
7. Xie R J, Hirosaki N, Kimura N, Sakuma K, Mitomo M. 2-phosphorconverted white light-emitting diodes using oxynitride/nitride phosphors. Applied Physics Letters, 2007, 90(19): 191101–

191103

8. Khoshnegar M, Sodagar M, Eftekharian A, Khorasani S. Design of a GaN white light-emitting diode through envelope function analysis. IEEE Journal of Quantum Electronics, 2010, 46(2): 228–237
9. Anikeeva P O, Halpert J E, Bawendi M G, Bulović V. Electroluminescence from a mixed red-green-blue colloidal quantum dot monolayer. Nano Letters, 2007, 7(8): 2196–2200
10. Schubert E F, Kim J K. Solid-state light sources getting smart. Science, 2005, 308(5726): 1274–1278
11. Chen C H, Su Y K, Sheu J K, Chen J F, Kuo C H, Lin Y C. Nitride-based cascade near white light-emitting diodes. IEEE Photonics Technology Letters, 2002, 14(7): 908–910
12. Ozden I, Makarona E, Nurmikko A V, Takeuchi T, Krames M. A dual-wavelength indium gallium nitride quantum well light emitting diode. Applied Physics Letters, 2001, 79(16): 2532–2534
13. Park K, Kwon M K, Cho C Y, Lim J H, Park S J. Phosphor-free white light-emitting diode with laterally distributed multiple quantum wells. Applied Physics Letters, 2008, 92(9): 091110–091112
14. Shei S C, Sheu J K, Tsai C M, Lai W C, Lee M L, Kuo C H. Emission mechanism of mixed-color InGaN/GaN multi-quantum-well light-emitting diodes. Japanese Journal of Applied Physics, 2006, 45(4): 2463–2466
15. Rostami A, Rasooli Saghai H, Baghban Asghari Nejad H. A proposal for enhancement of optical nonlinearity in GaN/AlGaN centered defect quantum box (CDQB) nanocrystal. Solid-State Electronics, 2008, 52(7): 1075–1108
16. Lai C Y, Hsu T M. Polarization field effect on group III-nitride semiconductors. Dissertation for the Doctoral Degree. Taiwan, China, 2003
17. Winkelnkemper M, Schliwa A, Bimberg D. Interrelation of structural and electronic properties in $In_xGa_{1-x}N$/GaN quantum dots using an eight-band $k \cdot p$ model. Physical Review B: Condensed Matter and Materials Physics, 2006, 74(15): 155322–155333
18. Wu Y R, Lin Y Y, Huang H H, Singh J. Electronic and optical properties of InGaN quantum dot based light emitters for solid state lighting. Applied Physics, 2009, 105: 13117–13123
19. Ranjan V, Allan G, Priester C, Delerue C. Self-consistent calculations of the optical properties of GaN quantum dots. Physical Review B: Condensed Matter and Materials Physics, 2003, 68(11): 115305–115311
20. Sakamoto A, Sugawara M. Theoretical calculation of lasing spectra of quantum-dot lasers: effect of homogeneous broadening of optical gain. IEEE Photonics Technology Letters, 2000, 12(2): 107–109
21. Sugawara M. Self-Assembled InGaAs/GaAs Quantum Dots. London: Academic press, 1999
22. Asada M, Miyamoto Y, Suematsu Y. Gain and the threshold of three-dimensional quantum-box lasers. IEEE Journal of Quantum Electronics, 1986, QE-22(9): 1915–1921
23. Fairman H S, Brill M H, Hemmendinger H. How the CIE 1931 color-matching functions were derived from Wright-Guild data. Color Research and Application, 1998, 22(1): 11–23
24. Han D S, Asryan L V. Output power of a double tunneling-injection quantum dot laser. Nanotechnology, 2010, 21(1): 15201–15214
25. Schubert E F, Gessmann T, Kim J K. Light-Emitting Diodes. Cambridge: Cambridge University Press, 2003